Liquid Crystals
Publication details, including instructions for authors and subscription information:
http://www.informaworld.com/smpp/title~content=t713926090

An addressing effective computer model for surface stabilized ferroelectric liquid crystal cells

P. Maltese[a]; R. Piccolo[b]; V. Ferrara[a]
[a] Department of Electronic Engineering, La Sapienza University, Roma, Italy [b] Department of Physics, University of Bari, Bari, ITALY

To cite this Article Maltese, P. , Piccolo, R. and Ferrara, V.(1993) 'An addressing effective computer model for surface stabilized ferroelectric liquid crystal cells', Liquid Crystals, 15: 6, 819 — 834
To link to this Article: DOI: 10.1080/02678299308036502
URL: http://dx.doi.org/10.1080/02678299308036502

LIQUID CRYSTALS, 1993, VOL. 15, NO. 6, 819–834

An addressing effective computer model for surface stabilized ferroelectric liquid crystal cells†

by P. MALTESE*‡, R. PICCOLO§ and V. FERRARA‡

‡ Department of Electronic Engineering, La Sapienza University, Via Eudossiana 18, 00184 Roma, Italy

§ Department of Physics, University of Bari, Via Amendola 173, 70126 Bari, Italy

(*Received 24 June 1992; accepted 24 June 1993*)

A simple uniform director model is discussed which provides, for the first time, an agreement with experimental data for the dynamic optical behaviour of SSFLC cells subject to matrix addressing waveforms. Its use in fast running, interactive software has enabled us to design new, high speed matrix addressing schemes which have been experimentally tested.

1. Introduction

For a bistable cell, such as the SSFLC cell [1], matrix addressing consists of controlling, in a short time window, the states latched by the M pixels in a particular row. This results from the application of a row selection waveform in combination with the data waveforms applied to the M columns. In N such consecutive addressing time windows the entire $N \times M$ panel can be written. The internal memory makes the contrast independent of N. The short line addressing times available from the SSFLC cells make TV complexity and TV rate refreshing possible. In contrast, using standard nematic cells, without electronic switches incorporated into each cell, the optical contrast is severely reduced for large values of $N (N > 50)$.

Many different matrix addressing techniques have already been presented and many more have been tested for the SSFLC display cell. However, the simple accepted rule that state changing occurs when a critical voltage–time pulse area is reached [2] can only explain in part a class of 'normal' or 'low voltage' addressing modes [3]. Only recently has a dynamic model for addressing been introduced that clarifies the main addressing properties of SSFLC cells [4] and in particular their high voltage limits [3, 5, 6], which have been found to be related to the biaxial properties of the dielectric tensor.

As in the first description of the SSFLC cell [1], a uniform director and tilted smectic layers were assumed. The latter assumption is the simplest one which takes into account the effects of the chevron structure of the layers [7]. A simple dynamic equation making use of a single state variable was obtained by considering the dielectric, polarization and viscosity torques and by adding the simplest possible heuristic expression for the elastic torque, the importance of which is only secondary when large voltages are used to obtain fast addressing.

* Author for correspondence.

† Presented at the Fourteenth International Liquid Crystal Conference, 21–26 June 1992, University of Pisa, Italy.

0267–8292/93 $10·00

High frequency (hf) stabilization in the addressing of SSFLC cells was first reported by Sato *et al.* [8] and is at the origin of special addressing modes such as the one reported by Wakira [9].

Leading pulse latching at high voltage was first reported as a speed limiting phenomenon in 'normal', i.e. 'low voltage' matrix addressing [6]. Experimental studies were reported by Maltese *et al.* [3] and by Hughes *et al.* [10] both of whom proposed new high voltage addressing modes and discussed other related phenomena such as hf stabilization.

The existence of a minimum pulse duration in the voltage–time (V–t) curves for state changing, first reported by Ohrihara [11], was studied in detail by Saunders *et al.* [5] giving rise to a new class of monopolar pulse high voltage addressing modes [12, 13].

Until now these three effects have been reported only for SSFLC cells having the chevron structure. They can be seen to be responsible for some fundamental phenomena which must be reproduced by a dynamic model of the SSFLC cell for it to be able to include the large number of known addressing schemes.

This paper reports how our model reproduces these three fundamental phenomena and describes the operation of the fast running, interactive software which we have developed to perform dynamic simulations of addressing schemes in the cells.

Finally, the paper describes the way in which our model has been able to reproduce all known addressing schemes and allows us to derive new performing schemes, which have been experimentally tested.

2. The model

A picture of the SSFLC cell and its electro-optical behaviour is shown in figure 1. In the chiral smectic C (S_C^*) phase, the liquid crystal director **n** lies along the surface of a cone defining an angle $\theta \approx 15$–$45°$ normal to the smectic layers. Let us assume, without loss of generality, that the cell walls are horizontal. In the cell the smectic layers are broken into chevrons and tilted from the vertical at an angle $\delta = 0{\cdot}8\theta$–$0{\cdot}9\theta$. In special cases smaller or even zero values can be obtained for δ, corresponding to quasi-bookshelf or ideal bookshelf structures. The director can be switched between two approximately horizontal surface stabilized positions by pulsed voltages, since the pulsed field couples with the spontaneous polarization of the liquid crystal ($P_s = 1$–$100\,\mathrm{nC\,cm^{-2}}$). The optical behaviour is approximately that of a birefringent slab the axes of which can rotate in the cell's plane through an angle $< 2\theta$. Crossed polarizers can extinguish the light in one state and transmit light in the other.

If the director is assumed to be symmetrical in each half cell, and only the optical behaviour for perpendicular view is considered, the chevrons in figure 1 can be reduced to the tilted smectic layers in figure 2. The angle ϕ of the director around the cone and the in-plane twist ω of the director are also defined in figure 2.

If the director is assumed to be uniform, the state of the cell is identified by the single parameter $\phi(t)$. The light transmission $L(t)$ between crossed polarizers rotated by $\pi/8$ is

$$L(t) = \tfrac{1}{2}(1 + \sin 4\omega)\sin^2(\rho/2), \tag{1}$$

where ρ is the optical retardation angle and the in-plane twist ω is given by:

$$\tan\omega = \frac{\sin\phi\tan\theta}{\cos\delta + \sin\delta\tan\theta\cos\phi}. \tag{2}$$

For simplicity, we assumed $\rho = \pi$ in our optical calculations.

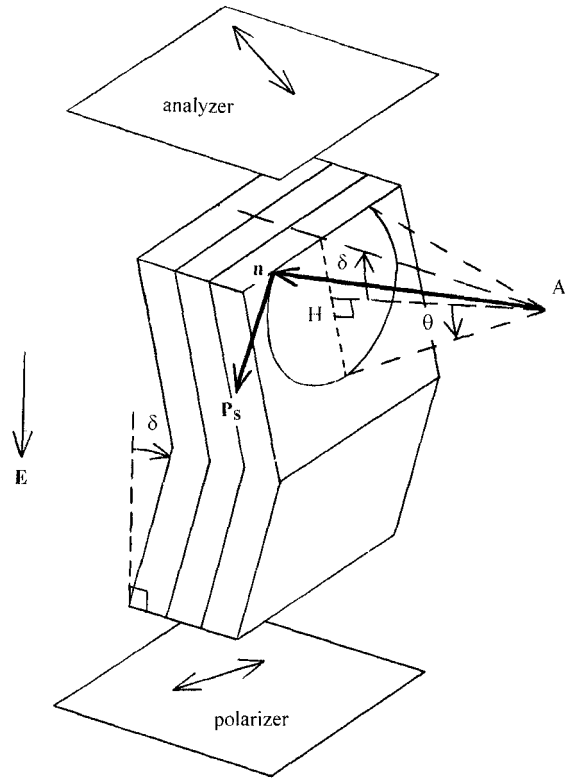

Figure 1. The SSFLC cell and the chevron structure of the S_C^* layers. The director **n** makes the characteristic angle θ to the layer normal AH, inclined at an angle δ to the cell walls. The vertical electric field **E** couples with the spontaneous polarization $\mathbf{P}_s$, which is orthogonal to **n**, lies in the plane of the layers and is tangential to the circle.

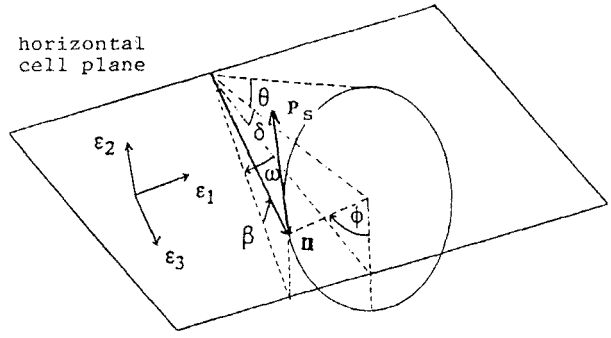

Figure 2. Simplified model with layers tilted at an angle δ and uniform director **n**. The rotation of **n** along the cone through an angle ϕ implies an in-plane twist ω and an out-of-plane tilt β (referring to a plane parallel to the cell walls). The biaxial dielectric tensor is characterized by the three constants ε_1, ε_2 (along $\mathbf{P}_s$) and ε_3 (along **n**). The dielectric anisotropy and the dielectric biaxiality are defined as $\Delta\varepsilon = \varepsilon_3 - \varepsilon_1$ and $\partial\varepsilon = \varepsilon_2 - \varepsilon_1$, respectively. We also introduce the effective dielectric biaxiality $\varepsilon_\Delta = \partial\varepsilon - \Delta\varepsilon \sin^2\theta$.

Tough, crude, uniform director models have been generally used to compute switching times and model the optical behaviour of the SSFLC cell [5, 14–17]. Their ability to predict more complex addressing phenomena has been shown only recently [4].

When considering only the main effect [1], which is derived from the balance of the viscous torque ($Q_v = -\eta_c d\phi/dt$) and the polarization torque ($Q_p = (P_s V(t)/d)\cos\delta\cos\phi$) acting on the director, we obtain

$$\frac{d\phi}{dt} = \frac{V(t)}{A}\cos\phi(t), \tag{3}$$

where $A = \eta_c d/(P_s \cos\delta)$, d being the cell thickness and $\eta_c = \eta \sin^2\theta$ [18] is the rotational viscosity of the **n** projection on to the smectic planes.

This equation is often used to describe the switching behaviour of the cell neglecting, in a first order approximation, the usually much smaller elastic and dielectric torques. However, as already recognized by Escher *et al.* [16], equation (3) cannot at all describe the matrix addressing properties of the SSFLC cells. In fact, for any equation of the form

$$\frac{d\phi}{dt} = f(\phi)V(t) \tag{4}$$

it follows:

$$\int_{\phi_0}^{\phi} \frac{d\phi}{f(\phi)} = g(\phi) - g(\phi_0) = \int_0^t V(t)\,dt. \tag{5}$$

where the left hand equality defines a new state variable [19] $g(\phi)$ which can have a one-to-one correspondence with ϕ.

Unlike $\phi(t)$, $g(t)$ has a linear system [19] dependence on the input variable $V(t)$, i.e. a dependence where the superposition principle is respected. Such a dependence of the cell state on $\int V(t)\,dt$ makes DC balanced data waveforms in each addressing window necessary. If not, in the absence of selection voltages, it would be impossible to maintain the selected state of a pixel during many addressing windows, in the presence of a data-dependent voltage addressing the other pixels in the same column, and this would result in long term bistability being destroyed. This is considered true even if equation (3) is only approximately respected.

However, if equation (3) were exact, it would follow from equation (5) that it is impossible to select one state or the other by the superposition of a given selection waveform, applied to the rows, and one or the other of two different DC balanced data waveforms, applied to the columns. This means that it would be impossible to effect matrix addressing. In fact the addition to a selection voltage of DC balanced data pulses would not change the right hand side of equation (5) at the end of the addressing window and no effect would be produced on he state of the cell.

A saturation in the optical response is experimentally observed if $|\int V(t)\,dt| > A_c$, where A_c is a critical pulse area, together with state latching when $\pm A_c$ is exceeded. The simplest model able to predict addressing [20], is obtained by introducing a saturation in the response given by equation (5). The addressing modes predicted are the ones previously explained in terms of critical pulse area, and named 'low voltage' or 'normal' addressing modes [3, 20].

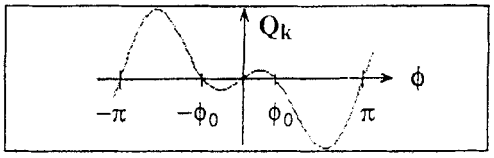

Figure 3. The simplest possible analytic function, for a heuristic elastic torque Q_k, giving a bistable SSFLC cell. $Q_k \propto (\sin 2\phi - 2\cos\phi_0 \sin\phi)$.

A better approach to explain the fundamental effects, in which we are interested, is the addition to equation (3) of the simplest possible expressions of the other usually smaller real torques acting on the director.

In the simulation, to make the cell relax when no voltage is applied and to render it bistable, an elastic torque Q_k is necessary which crosses the zero in two relaxed states. During the selection pulses, this torque is much smaller than the others, so that its exact expression is not needed to correct equation (3). In a uniform director model, elastic torque can only be included in a form physically corresponding to a rigid liquid crystal, in which the director is elastically coupled to the boundary surfaces. As in Escher *et al.* [17], we introduce arbitrarily in the model an elastic torque according to its simplest possible symmetric expression. This is plotted in figure 3 and corresponds to

$$Q_k = (\eta_c/T_r)(\sin 2\phi - 2\cos\phi_0 \sin\phi), \tag{6}$$

where $+\phi_0$ and $-\phi_0$ characterize the two stable configurations and T_r is an observable relaxation time constant, introduced here in its ratio with the viscosity (an independently observable quantity), to describe the overall effective elastic behaviour of the cell.

To explain the high voltage phenomena, we computed the V^2 dependent torque Q_e from a biaxial dielectric tensor [4]. In agreement with Jones *et al.* [14] (while using our definition for ϕ), we can express it as

$$Q_e = \frac{\varepsilon_0 \varepsilon_\Delta V^2}{2d^2} \cos^2\delta(\sin 2\phi - 2\cos\phi_v \sin\phi), \tag{7}$$

where we have introduced the effective relative dielectric biaxiality of the liquid crystal, defined as

$$\varepsilon_\Delta = \partial\varepsilon - \Delta\varepsilon \sin^2\theta \tag{8}$$

in which $\Delta\varepsilon = \varepsilon_3 - \varepsilon_1$ is the anisotropy and $\partial\varepsilon = \varepsilon_2 - \varepsilon_1$ is the biaxiality, defined as usual [14] (see figure 2).

In equation (7), $+\phi_v$ and $-\phi_v$ represent the angles for which $Q_e = 0$, i.e. the limit equilibrium values assumed by ϕ for infinite voltage, when Q_e is dominant. ϕ_v is

$$\cos\phi_v = -\frac{\Delta\varepsilon \sin 2\theta \tan\delta}{2\varepsilon_\Delta} \tag{9}$$

and is equal to $\pi/2$ for $\Delta\varepsilon = 0$ and in bookshelf cells. For chevron cells it becomes somewhat different from $\pi/2$, being smaller for a negative dielectric anisotropy. This is the most common case, even if for large $|\Delta\varepsilon/\varepsilon_\Delta|$ the expression (6) can correspond to non-real ϕ_v [20].

For positive ε_Δ, the cell has hf stabilization (as always happens [20]), and the dynamic equation

$$\eta_c \frac{d\phi}{dt} = Q_p + Q_e + Q_k \tag{10}$$

can be normalized by defining, for the cell, a real positive characteristic voltage (for hf stabilization) V_c, a characteristic time $T_c = A/V_c$ and a constant $\lambda = (T_r/2T_c)^2$ [4]. In physical terms, V_c is given by

$$V_c = \frac{d}{\cos\delta}\sqrt{\left(\frac{2\eta_c}{\varepsilon_0 \varepsilon_\Delta T_r}\right)}. \tag{11}$$

Its magnitude is related to the hf stabilization of the cell. In fact, if only a very high frequency voltage is applied, with rms amplitude V_{hf} and zero mean value, the equilibrium angle around which ϕ oscillates corresponds to $Q_e + Q_k = 0$ (since the average values of Q_v and Q_p are zero) and is given by

$$\cos\phi = \frac{V_c^2 \cos\phi_0 + V_{hf}^2 \cos\phi_v}{V_c^2 + V_{hf}^2}. \tag{12}$$

In terms of a reduced voltage $V' = V/V_c$ and a reduced time $t' = t/2T_c$, then equation (10) can be rewritten as

$$\frac{d\phi}{dt'} = V' \cos\phi \left[1 + (\sin\phi - \cos\phi_0 \tan\phi)\frac{1}{V'\sqrt{\lambda}} + (\sin\phi - \cos\phi_V \tan\phi)\frac{V'}{\sqrt{\lambda}}\right]. \tag{13}$$

This simple, phenomenological equation is able to explain the occurrence of a minimum pulse duration for latching with monopolar pulses, to reproduce both trailing and leading pulse latching as well as to describe complex addressing phenomena in terms of simple liquid crystal and cell properties [4].

As can be seen from equation (13), $V_c/\sqrt{\lambda}$ and $V_c\sqrt{\lambda}$ represent the approximate limits for V between which both the elastic and dielectric torques can be considered smaller than the polarization torque so that equation (3) is approximately valid to describe switching, even though not so far for matrix addressing. In a logarithmic voltage scale, λ measures the width of such a voltage range, centred around V_c, inside which the linear system state equation (5) is approximately valid and the switching time is inversely proportional to the applied voltage. For this reason we termed λ the 'voltage linearity range' [4].

An example of a plot of the right hand term in equation (13), in the region of our interest for ϕ, and for large positive reduced voltages V', is shown in figure 4. For our typical chevron cell $\phi_0 = 0{\cdot}4$ rad, $\phi_v = 1{\cdot}2$ rad, $\lambda = 10$ (see discussion in the following section). For different values of the parameters, the general shape of the curves remains the same. The curves for negative voltages are symmetric to the ones shown.

The curve for $V' = 0$ only corresponds to the elastic torque (compare figure 3). Between $+\phi_v$ and $-\phi_v$, the reduced rate of change of ϕ becomes always positive (in the range $-\pi/2 < \phi < \pi/2$) when increasing V' over small values and remains so until $V' \cong 9$. Over this voltage, square wave switching becomes impossible. However, for negative angles, corresponding to the start of the switching process, the rate of change starts to decrease when $V' \cong 5$. The asymmetry between the left and right side of the curves makes high voltage addressing modes possible at even lower selection voltages. To exploit this asymmetry, at best bipolar data should be applied, when the selection voltage changes sign and $\phi \cong \pm\pi/4$, as in the operation of the addressing modes that make use of stop pulses [3].

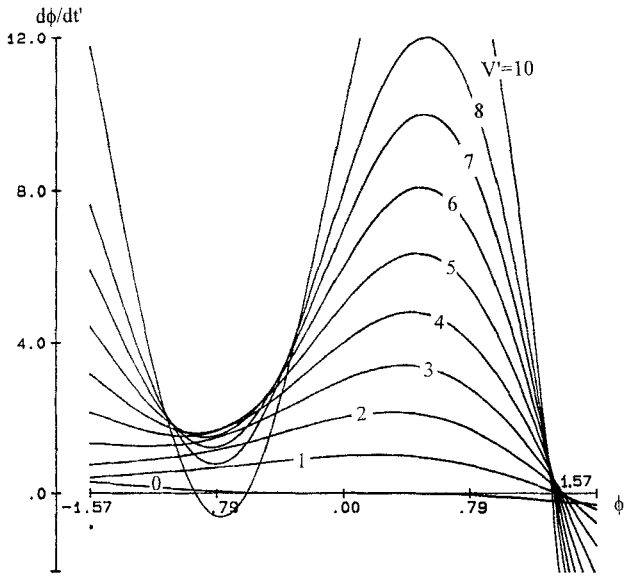

Figure 4. Plot of $d\phi/dt'$ as a function of ϕ for different values of V' corresponding to the differential equation (13), to which the addressing behaviour of the SSFLC cell is reduced, in the case $\phi_0 = 0{\cdot}4$ rad, $\phi_v = 1{\cdot}2$ rad and $\lambda = 10$.

3. Switching simulation

By changing δ, ϕ_0 and ϕ_v, the numeric model gives computed results $\phi(t)$ and $L(t)$ which should be equally valid for chevron, quasi-bookshelf and bookshelf structures. However, due to the absence of comparable experimental results in the literature we focused our attention on the computer simulation of cells having the chevron structure. We used $\theta = \pi/8$ rad, $\delta = 0{\cdot}9\,\theta$, and $\phi_0 = 0{\cdot}4$ rad as typical values for the chevron cells for most of our calculations.

Our first aim was to find, in our model, the previously identified main addressing phenomena for chevron-layered cells. To do this we performed simulations of the response to monopolar and bipolar latching pulses of varying reduced duration and amplitude. By so doing, different universal threshold curves were obtained for each value of λ. Since a positive dielectric biaxiality and not a non-zero dielectric anisotropy is necessary to explain hf stabilization and minimum switching times in V_s–T_s curves [21], we assumed, at first, that the dielectric anisotropy was zero, so that $\phi_v = \pi/2$. For positive real V_c, a non-zero positive effective dielectric biaxiality is inherent in equation (13).

The results from these computer simulations are plotted in figures 5 and 6, where the reduced switching times are plotted against the corresponding reduced switching voltages. For any given λ, latching occurs between a minimum voltage and a maximum voltage, both of which correspond to vertical asymptotes of the curves, and are the same for monopolar and bipolar pulses. Their ratio is proportional to the voltage linearity range λ, which can roughly be considered to be representative of the voltage range in which switching occurs in the model and, for monopolar pulses, $T_s \propto 1/V_s$. As is well known, in place of the minimum switching voltage, a different regime of wall motion assisted switching is experimentally observed.

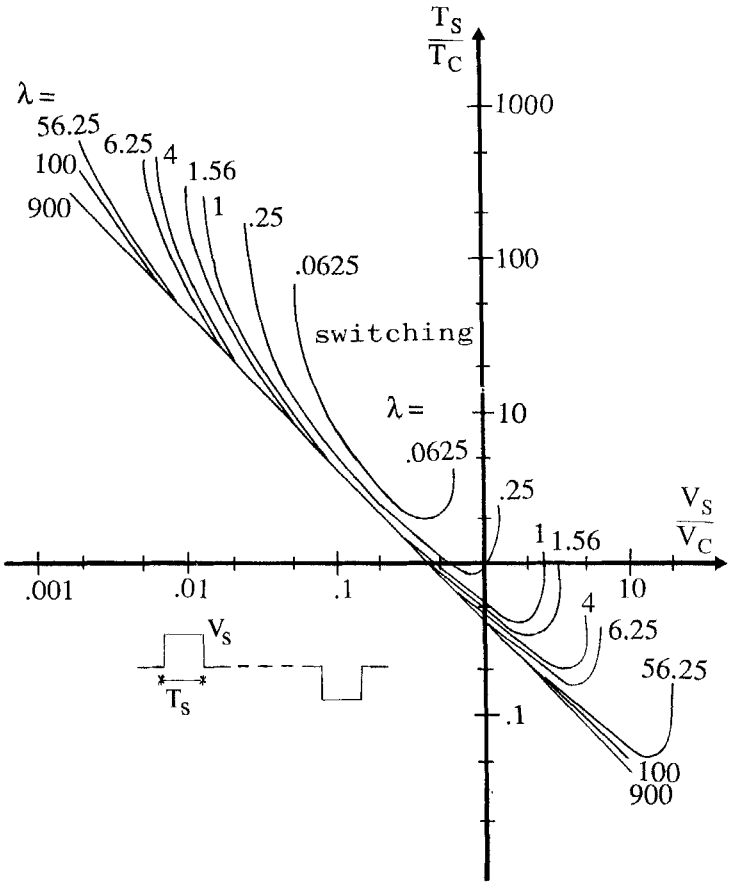

Figure 5. Universal switching curves giving the switching threshold for monopolar pulses in SSFLC cells. T_c and V_c are the characteristic time and voltage, respectively. T_s and V_s are, respectively, the threshold duration and amplitude of the voltage pulses required to make the cell change state. λ is the voltage linearity range of the cell. $\phi_0 = 0{\cdot}4$ rad, $\phi_v = \pi/2$.

In the case of bipolar pulses, the computed latching region is divided into two parts by an intermediate boundary (with an asymptotic voltage 1·5–4 times smaller than the maximum voltage for switching). The low voltage branches of the threshold curves correspond to trailing pulse latching. Their positions are above the corresponding curves for monopolar pulses and their smaller slopes, fit the experimental data [3, 10]. The smaller, high voltage regions correspond to leading-pulse latching (used in the inverted Seiko addressing mode) and fit the experimental data [3, 9]. However this region is only wide enough for excessive values of λ, corresponding to hf stabilization effects much larger than those experimentally observed.

For lower λ. however, the proper width of the region is found if a negative dielectric anisotropy, corresponding to smaller values of ϕ_v, is taken into account. The importance of this high voltage limit angle is shown by figure 7, in which, for $\lambda = 10$, we plotted four different cases. For constant λ, the position of the minimum switching time for monopolar pulses appears to be strongly dependent on the dielectric anisotropy and even more the extension of the leading-pulse switching region. The experimental data are best fitted by curve c, corresponding to $\phi_v = 1{\cdot}2$ rad. Also from the literature

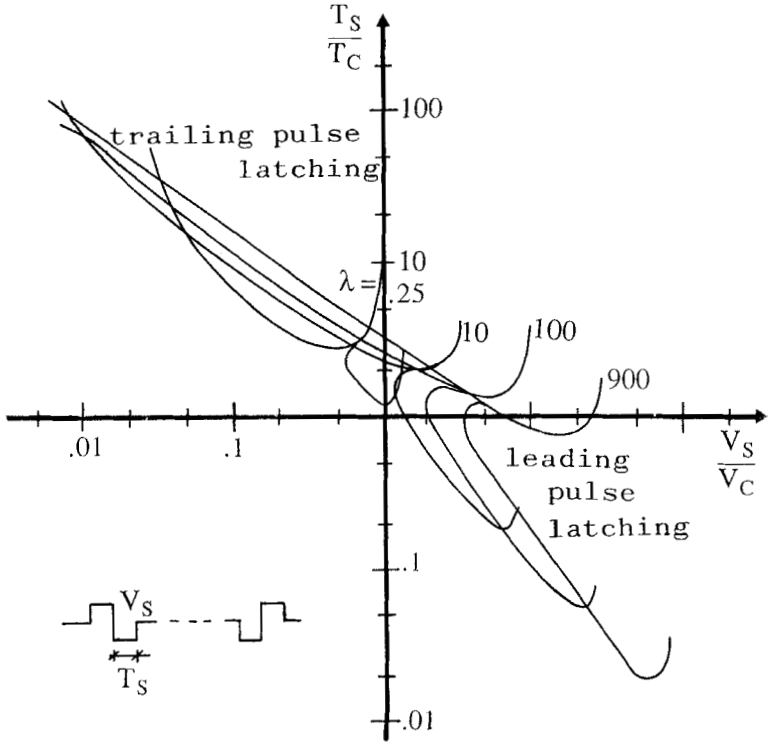

Figure 6. Universal switching curves giving the switching thresholds for bipolar pulses in the leading and trailing pulse latching modes. $\phi_0 = 0{\cdot}4$ rad, $\phi_v = \pi/2$.

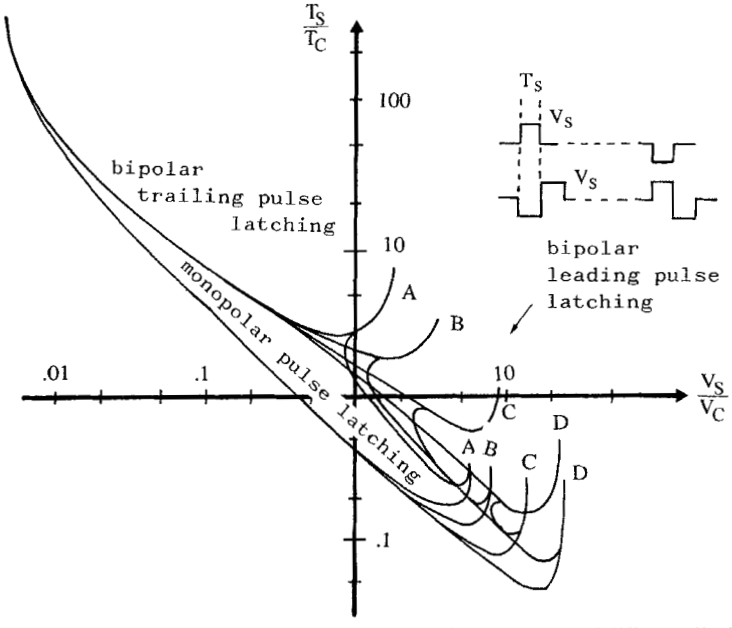

Figure 7. Computed effect, which is large in the high voltage region, of different limit angles ϕ_v on the universal switching curves. $\phi_0 = 0{\cdot}4$ rad, $\lambda = 10$. $\Delta\varepsilon > 0$: (A) $\phi_v = 1{\cdot}9$. (B) $\phi_v = \pi/2$. $\Delta\varepsilon < 0$: (C) $\phi_v = 1{\cdot}2$, (D) $\phi_v = 0{\cdot}9$.

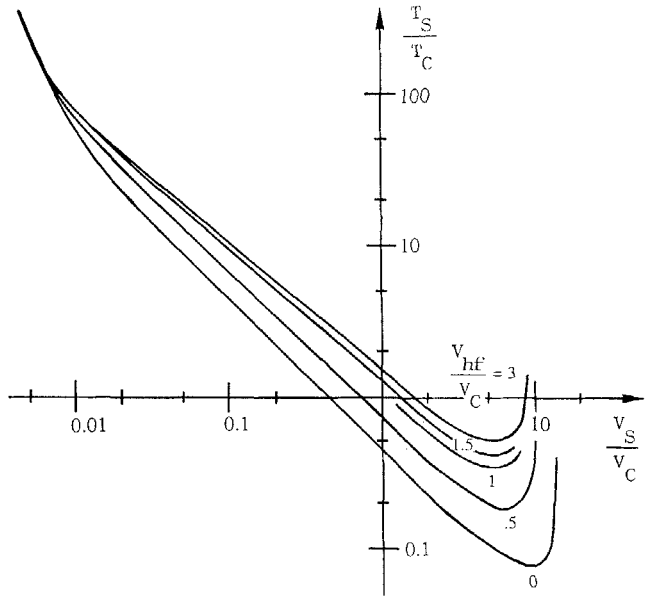

Figure 8. Effect of high frequency voltages between the pulses on the switching threshold for monopolar pulses. $\phi_v = 1{\cdot}2$, $\phi_0 = 0{\cdot}4$ rad, $\lambda = 10$.

[12, 20], biaxial dielectric constants giving values close to $\phi_v = 1{\cdot}2$ rad are found, leading us to adopt this value for most calculations.

Figure 8 shows, for $\phi_v = 1{\cdot}2$ rad, the effect in the model, on the switching threshold curves, of hf stabilization voltages of amplitude V_{hf} applied to the cell between monopolar pulses, by fitting the experimental data from Saunders [5]. If a zero (or positive) dielectric anisotropy were taken into account in the model, excessive effects would result.

4. Interactive computing procedure

We have derived an interactive computer program from the model in order to use it as a working instrument to define the appropriate waveforms and to adjust the operational conditions of different addressing modes in as short a time as possible. The input data were as follows: the selection (or row) waveform; the data (or column) waveform in each addressing time window; the black, white or intermediate values of the pixels to be consecutively addressed in the same column; and the amplitudes of both voltage waveforms to be combined. To characterize the cell, the cone angle θ, the tilt angle δ and the stable value ϕ_0 of the state variable ϕ were assigned. The other necessary parameters can be assigned to one of the following two sets:

(i) a reduced parameter set with ϕ_v, V_c, T_c and λ, which characterize the global addressing behaviour of the cell;

(ii) a material parameter set with cell thickness d, η_c, the biaxiality $\partial\varepsilon$, the anisotropy $\Delta\varepsilon$, the relaxation time constant T_r and spontaneous polarization P_s.

The operation of a full menu in the program allowed the variation of any one of these parameters and the immediate observation of the corresponding result. The data and selection voltage waveforms, as well as the corresponding optical outputs, could be plotted on the screen and printed with the corresponding numerical values.

5. Addressing simulation

A large number of simulations were performed with the complex voltage waveforms actually used in most of the different addressing techniques so far reported, in order to compare them with the results from our model. By so doing, it was possible to confirm the existence in the model of all the addressing schemes tested. Computer simulations of two well-known advanced addressing modes are shown as examples in figures 9 and 10.

After writing the data files describing a given addressing scheme, the row voltages, the data voltages and the time scales for which the addressing mode eventually operated correctly had to be adjusted, through several computer simulations guided by our experimental experience. Correct operation means that different latched outputs were obtained as a response to changes in a single relevant data window, independently of any change in other data windows or in the initial state of the cell. After this lengthy procedure, operating ranges were almost always found for our standard values of $\lambda = 10$ and $\phi_v = 1{\cdot}2$ rad. Only a few cases required a larger ϕ_v (1·4 rad) in order to find an existing operating region.

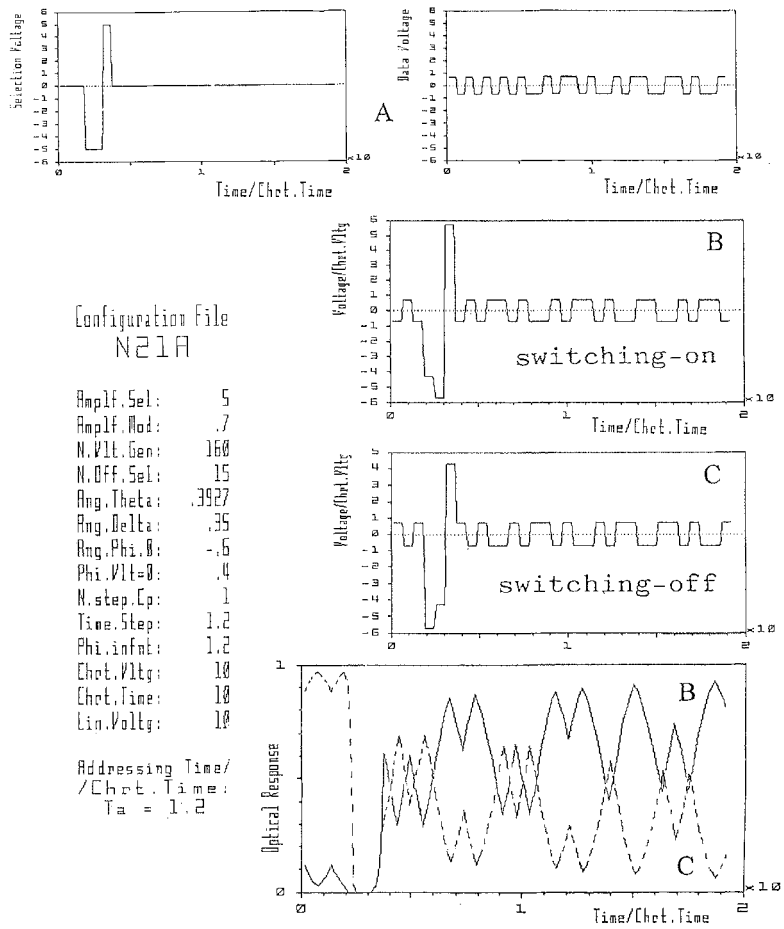

Figure 9. Addressing simulation of the 'normal' LETI-BARI scheme [3]; (A) selection and worst data voltages applied, respectively, to the rows and to the columns of the matrix; (B) worst case switching on; (C) worst case switching off.

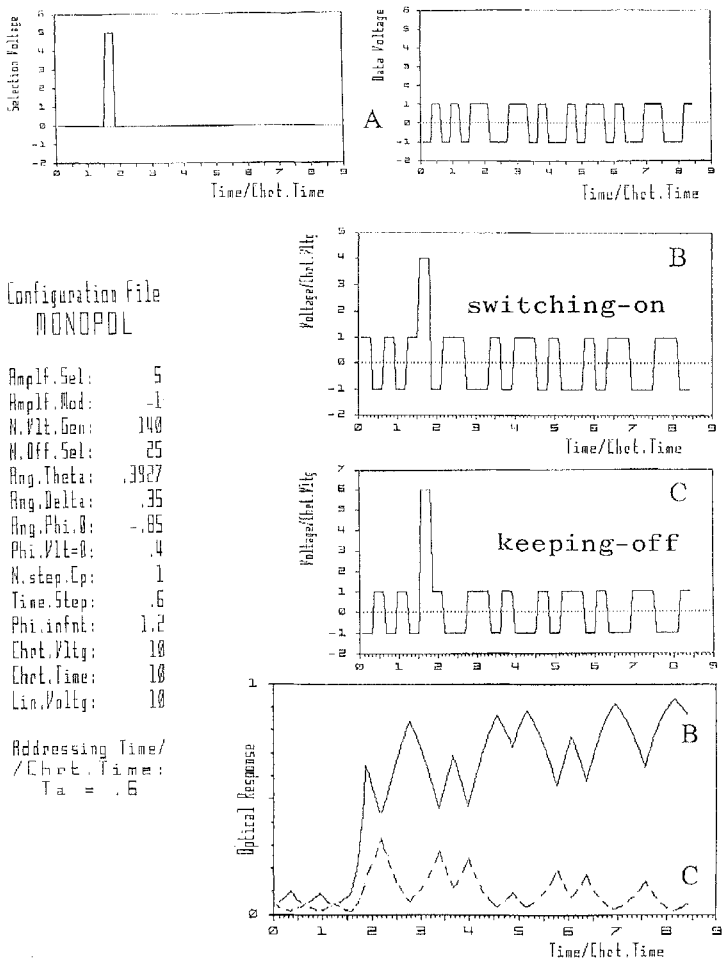

Figure 10. Addressing simulation of the high voltage monopolar JOERS Alvey scheme [12]. (A); (B); (C) as in figure 9.

In the figures, which reproduce outputs from the computer program, state changes of the cell are shown with worst case data patterns in proximity to the high speed limits of the different addressing modes.

6. New addressing modes

The main purposes, for which our simulation software was designed, were to optimize the known addressing modes and to find new ones. The investigations started from the already reported class of 'fast' addressing modes [3]. They are characterized by the use of a stop pulse immediately after the write pulse, in the selection waveform, and of postcompensated bipolar pulses, in the data, in correspondence with the last part of the write pulse and with the stop pulse.

Bipolar erasing, in which writing is preceded by two longer erase voltage steps of opposite polarity, has been proposed by Maltese *et al.* [6], for the control of grey shades and has been used for this purpose by Hartman [22]. Our computer experiments have shown that shorter addressing times and better contrasts than with monopolar erasing

are also obtained. Moreover, in this way, DC free selection pulses can be employed, eliminating some inconveniences which are experimentally found otherwise (flicker, especially on moving edges, when the polarity is inverted at each frame).

Figure 11 shows a '4 6 3 1 fast mode' corresponding to one of our best results in double erase fast addressing. The step durations in the selection waveform are in the ratio 4/6/3/1. The duration of the addressing window, equal to the time shift between consecutively selected rows, is 2.

The computer simulation revealed significant improvements in the addressing speed if a long enough pause is inserted between the erasing portion and the write stop portion of the selection waveform. The relaxation occurring during the pause permits the use of much shorter write pulses, for a given 'high' voltage. For such 'pause fast' schemes, the best results are achieved with 4/6/pause/3/1 time ratios (see figure 12). The line addressing time so obtained is approximately a quarter of those for the LETI-BARI and JOERS Alvey addressing schemes (if the latter is corrected to take into account the need for double selection, as in the Seiko mode, with pulses of opposite polarity).

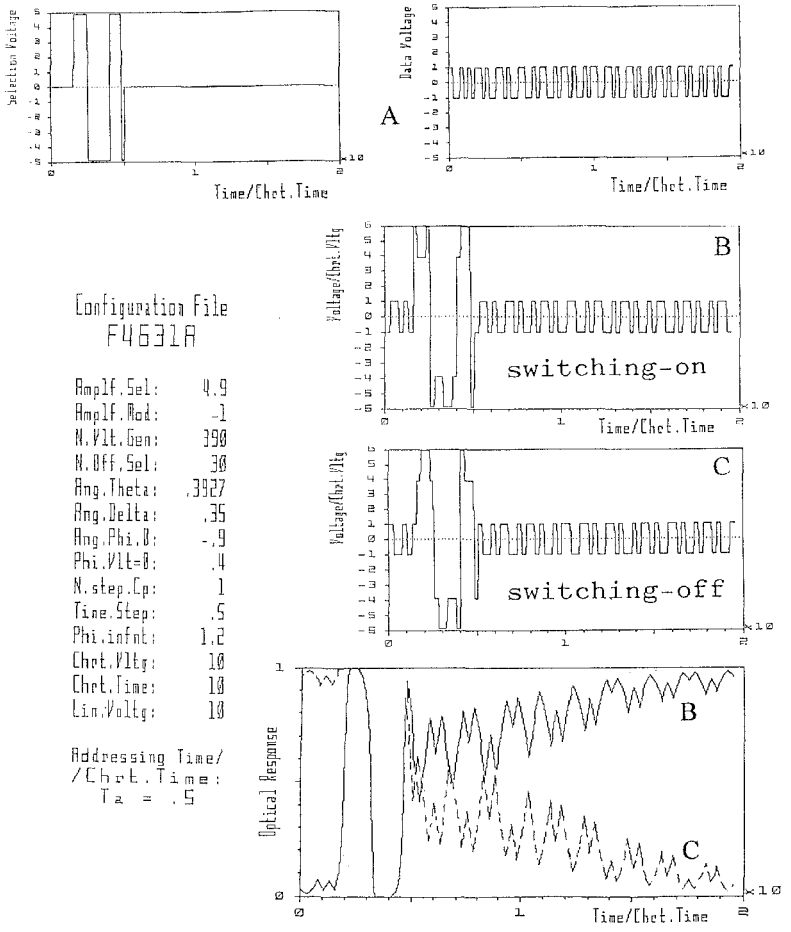

Figure 11. Addressing simulation of a new '4 6 3 1 fast mode' found with the aid of the computer model. (A); (B); (C) as in figure 9.

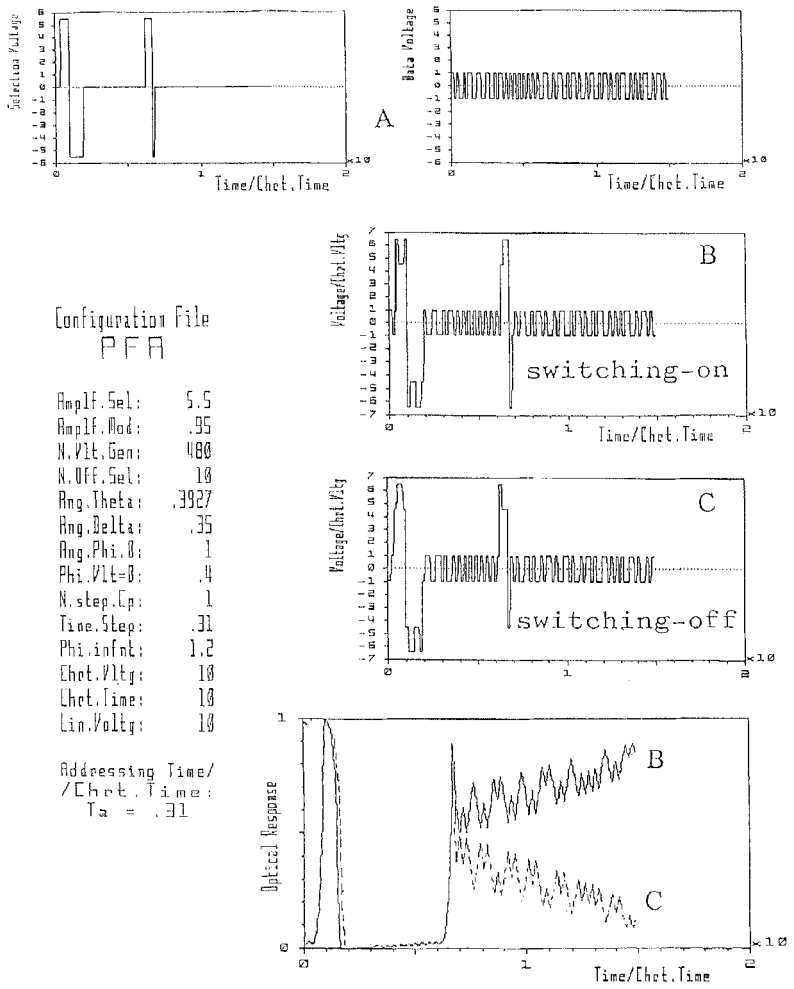

Figure 12. Addressing simulation of a new 'pause fast mode', found with the aid of the computer model, making use of step durations in the ratios 4/6/(pause)/3/1. (A); (B); (C) as in figure 9.

These results from the simulations were experimentally checked and found to be correct. Both the 4 6 3 1 fast mode and the 4 6 pause 3 1 fast mode have been implemented in test cells from GEC, filled with the low P_s liquid crystal Merck 90-917 ($P_s = 2{\cdot}9\,\text{nC cm}^{-2}$, $\Delta\varepsilon = -0{\cdot}9$) and measured at 40°C. The latter mode provided line addressing times shorter than any other.

The experimental records of two opposite state changes are plotted in figures 13 (A) and (B), in an expanded time scale of $100\,\mu\text{s div}^{-1}$, comparable to that of the computer plots. Only the data wavefronts (± 16 V) are plotted, which are different only in the $20\,\mu$s long addressing window. To demonstrate the overall effect, an off cell was switched on for four consecutive 10 ms refresh cycles and then switched off again, obtaining, at $5\,\text{ms div}^{-1}$, the plot in figure 13 (C). In this case, only the selection voltage is shown (as low as ± 38 V). In figure 13, the light outputs correspond to negative values measured from the central line of the screen.

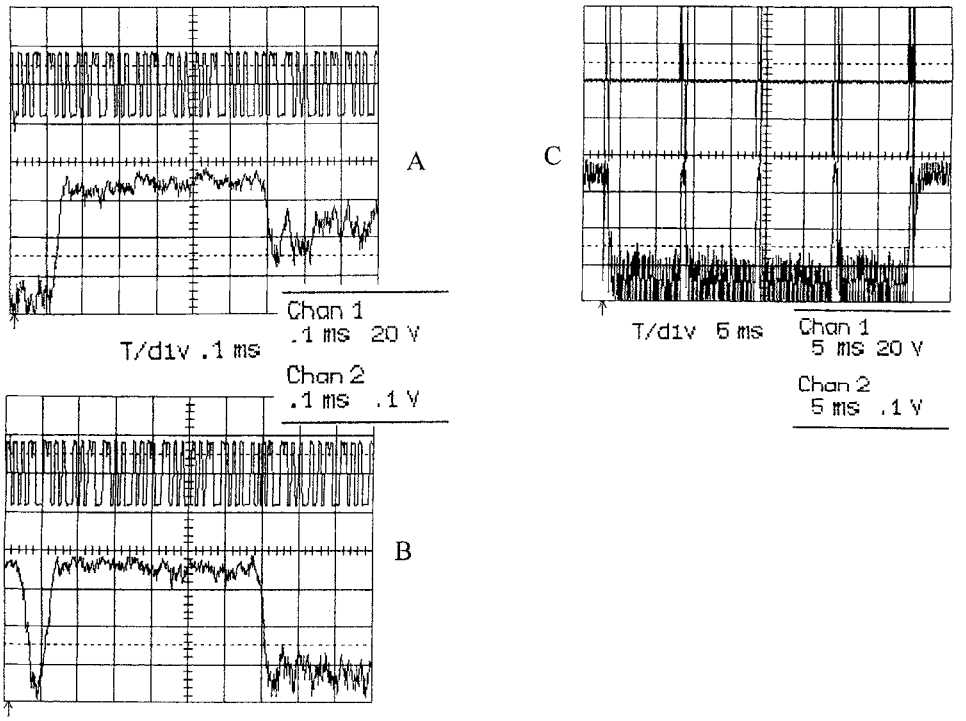

Figure 13. Experimental confirmation of the 4/6 pause/3/1 fast mode. Voltages: 20 V div^{-1}, Light output: arbitrary units, negative, zero on the central screen line; (A) and (B): switching on and switching off at 100 ms div^{-1}; (C) switching on for four refresh cycles at 5 ms div^{-1}.

7. Conclusions

Equation (13) describes complex addressing phenomena in terms of simple and measurable, but not commonly available, liquid crystal and cell properties.

The corresponding dynamic model, in the framework of an interactive simulation program, has been used to reproduce almost all the known addressing schemes and has proved to be very useful for the design of new ones, before confirming them experimentally. In fact, the model allows the setting up of ideal experiments in which the cell properties can be modified intentionally, but cannot be changed unintentionally, as a result of thermal cycles and applied voltages, as can occur in laboratory experiments.

Even though we are just beginning to develop its full potential, we are convinced that our model provides a powerful instrument for the design of improved addressing waveforms and cells with better addressing capabilities.

We gratefully acknowledge test cells from GEC, Wembley, UK and DRA, Malvern, UK, helpful discussion in the frame of the European project ESPRIT 2360 FELICITA, computer plots from A. Pontecorvo as well as financial support from the EEC in ESPRIT and from the Italian CNR in the National Project for Telecommunications.

References

[1] Clark, N. A., and Lagerwall, S. T., 1980, *Appl. Phys. Lett.*, **36**, 899.
[2] Lagerwall, S. T., Wahl, J., and Clark, N. A., 1985, *Proceedings of the International Display Research Conference*, San Diego, p. 213.

[3] MALTESE, P., DIJON, J., and LEROUX, T., 1988, *Proceedings of the International Display Research Conference*, San Diego, p. 98.
[4] MALTESE, P., 1991, *Proceedings of the International Display Research Conference*, San Diego, p. 77, also presented at the *Ferroelectric Liquid Crystal Conference*, O-34, Boulder, 1991.
[5] SAUNDERS, F. C., HUGHES, J. R., PEDLINGHAM, H. A., and TOWLER, M. J., 1989, *Liq. Crystals*, **6**, 341.
[6] MALTESE, P., DIJON, J., LEROUX, T., and SARRASIN, D., 1988, *Ferroelectrics*, **85**, 265.
[7] RIEKER, T. P., CLARK, N. A. SMITH, G. S., PARMAR, D. S., SIROTA, E. B., and SAFINYA, C. R., 1987, *Phys. Rev. Lett.*, **59**, 2658.
[8] SATO, Y., TANAKA, T., NAGATA, M., TAKESHITA, H., and MOROZUMI, S., 1987, *Proc. SID*, **28**, 189.
[9] WAKITA, N., UEMURA, T., OHNISHI, H., and OTHA, I., 1990, *Displays*, **11**, 32.
[10] HUGHES, J. R., and SAUNDERS, F. C., 1988, *Liq. Crystals*, **3**, 1401.
[11] ORIHARA, H., NAKAMURA, K., ISHIBASHI, Y., YAMADA, Y., YAMAMOTO, N., and YAMAWAKI, Y., 1986, *Jap. J. appl. Phys.*, **25**, L839.
[12] SURGUY, P. W. H., AYLIFFE, P. J., BIRCH, M. J., BONE, M. F., COULSON, I., CROSSLAND, W. A., HUGHES, J. R., ROSS, P. W., SAUNDERS, F. C., and TOWLER, M. J., 1991, *Ferroelectrics*, **122**, 63.
[13] YEOH, C. T. H., MOSLEY, A., LISTER, S. J. S., and NICHOLAS, B. M., 1991, presented at the *Ferroelectric Liquid Crystal Conference*, O-32, Boulder.
[14] JONES, J. C., TOWLER, M. J., and RAYNES, E. P., 1991, *Ferroelectrics*, **121**, 91.
[15] XUE JIU-ZHI, HANDSCHY, M. A., and CLARK, N. A., 1987, *Liq. Crystals*, **2**, 707.
[16] ESCHER, C., DUEBAL, H.-R., HARADA, T., ILLIAN, G., MURAKAMI, M., and OHLENDORF, D., 1991, *Ferroelectrics*, **113**, 269.
[17] JONES, J. C., and RAYNES, E. P., 1992, *Liq. Crystals*, **11**, 199.
[18] ESCHER, C., GEELHAAR, T., and BOHM, E., 1988, *Liq. Crystals*, **3**, 469.
[19] ZADEH, L. A., and DESOER, C. A., 1963, *Linear System Theory* (McGraw-Hill).
[20] MALTESE, P., 1992, *Molec. Crystals liq. Crystals*, **215**, 57.
[21] ELSTON, S. J., SAMBLES, J. R., and CLARK, M. G., 1990, *J. appl. Phys.*, **68**, 1242.
[22] HARTMAN, W. J. A. M., 1991, *Ferroelectrics*, **122**, 355.